A preliminary assessment of frozen-in offshore wind turbines

van der Stap, Florian L.; Nielsen, Martin B.; Hendrikse, Hayo

Publication date
2024

Document Version
Final published version

Published in
Proceedings of the 27th IAHR International Symposium on Ice (Gdansk, 2024)

IAHR AIRH
Hosted by Spain Water and IWHR, China

27th IAHR International Symposium on Ice
Gdańsk, Poland, 9 – 13 June 2024

A preliminary assessment of frozen-in offshore wind turbines

Florian L. van der Stap[1,2], Martin B. Nielsen[2], and Hayo Hendrikse[1]
[1] *Department of Hydraulic Engineering, Delft University of Technology, The Netherlands*
[2] *Wood Thilsted Partners, Copenhagen, Denmark*
fvs@woodthilsted.com, mbn@woodthilsted.com, h.hendrikse@tudelft.nl

Abstract: The frozen-in scenario – a condition where the offshore wind farm is fully enveloped by a large ice cover – is not typically considered during design. The current study explores this scenario by including a sufficiently large surrounding ice sheet, modelled as a representative linear elastic spring at mean sea level, in a dynamic model of an offshore wind turbine. The effects of the presence of ice on natural frequencies and flexibility of the offshore wind turbine is investigated, as well as its effect on load effects in typical wind-dominated design load cases. Emphasis is placed on cases governing the design of structures above waterline, such as extreme coherent gusts and directional changes. By varying the spring stiffness representing the ice, the load, deformation, and strain rate the modelled ice was subject to, were determined. The study found that the extreme overturning moment and damage equivalent moment reduce when the offshore wind foundations are surrounded by ice, whereas the shear increases from MSL and below. The combined load effects from the frozen-in load case show a higher utilization for a few select elevations below MSL. Depending on the assumed relationship between ice thickness and stiffness, the study evaluates the conditions under which the ice sheet could potentially grow and remain intact during both power production and extreme events. These findings indicate that based on the current methodology, the frozen-in load case cannot be disregarded and should be included in design in regions where there is an increased risk of encountering these conditions. However, it is expected that with improved ice modelling, accounting for viscoelastic behavior and ice failure, utilization levels would not exceed those observed in ice-free conditions.

Keywords: foundation design; load case; adfreeze; ice failure.

1. Introduction

With the expansion of the offshore wind industry into the Baltic Sea, the challenge of sea ice has solidified as an essential aspect of design. In the previous decade substantial research has been done on the impact of drifting sea ice, which may lead to ice-induced vibrations such as intermittent crushing and multi-modal interaction (Hammer et al., 2023; Sodhi, 1988). The occurrence of these interactions is dependent on the development of ice in- or outside of an offshore wind farm and the subsequent drifting of the ice sheet into the wind farm – given sufficient forcing from wind and current. However, the scenario in which ice grows locally in and around the wind farm and remains stationary under insufficient driving forces remains considerably less understood.

Such a situation is easily imagined if the offshore wind farm is near shore in a region prone to landfast ice formation. Nonetheless, a similar situation could occur if a sufficiently large floe forms in and around the ice farm, under insufficient driving forces, leading to stationary ice. These conditions are referred to as the 'frozen-in' load case here. One of the first mentions of stationary ice and the resulting loads, is in paper by Croasdale (1975), which discusses the potential of high forces when movements start up again due to the formation of an *"intimate contact condition"*. Notably, Croasdale commented that the South Beaufort Sea lacks sufficient tidal water level variations to prevent this frozen-in scenario. While this particular concern may not be relevant to the South Beaufort Sea, investigations into the frozen-in load case for offshore structures have predominantly centered on the loads due to stationary ice in tidal variations. This is because a vertically sided structure, when surrounded by stationary level ice in a location with large tidal variations, will be subject to large vertical forces (Kerr, 1975).

There are many reports of such vertical forces leading to (consecutive) uplift of the specific structure (Christensen & Tryde, 1984, 1986; Ohtsuki et al., 1988; Terahima et al., 2006). The vertical uplift force can be calculated exactly if the ice sheet is assumed to be an infinite elastic plate rigidly attached to structure as was done in the first papers addressing the issue (Kerr, 1975). In this analysis the vertical force is limited by the flexural strength of the ice, which can be further subdivided into radial and circumferential failure (Terahima et al., 2006). Early investigations also focused on the other typical failure mode of stationary ice during water level fluctuations: shear failure at the pile-ice interface (Sackinger & Sackinger, 1977). Experimental data confirmed that both failure modes were observed for ice in full contact with a vertically sided structure (Inoue & Frederking, 1986). Notably, their research highlighted significantly stronger adhesion —approximately 3.5 times higher — for fresh ice than saline ice, which is particularly relevant for the Baltic Sea given its brackish nature and the prevalence of fresher water in its northern regions. By comparing the maximum load of the two failure modes, the vertical force can be determined with the following equation (Terahima et al., 2006):

$$\frac{\sigma_f h}{\tau_B a} = \frac{2\pi}{1.154[1.05+2(\lambda a)+(\lambda a)^3/2]} \quad \textbf{[1]}$$

where σ_f is the flexural strength of the ice sheet, τ_B is the adfreeze bond strength between the surface of the structure and the ice sheet, h is the thickness of the ice sheet, a is the radius of the cross-section of the structure in the ice, and $\lambda = \sqrt[4]{\frac{\kappa_w}{D}}$, where κ_w is the self-weight of the water and D is the flat plate flexural rigidity of the ice sheet.

Further investigation into the frozen-in load case has led to the development of methods for the successive uplift due to the tidal variations rather than a single cycle (Christensen & Tryde,

1984) and methods for level ice sheets in contact with large vertical walls leading to extreme loads (Christensen & Tryde, 1986). Additionally, it was shown that allowing for partial flooding during water level fluctuations has a significant impact (Kerr & Stafford, 1986) as does the material of the structure, which has been shown to significantly impact the observed uplift due to the variability of the adfreeze strength (Ohtsuki et al., 1988). An extreme case of the frozen-in load case that was evaluated in research by Adachi examined the effects of an earthquake in stationary ice, suggesting this load case should not be ignored as the response shear force exceeded the ice crushing load (Adachi et al., 1988).

From the extensive research on the adfreeze topic formulations for load estimates have long been known and integrated into design standards such as ISO 19906 (2019) and IEC 61400-3-1 (2019). In addition to accounting for the vertical load induced by stationary ice, ISO 19906 prescribes the consideration of horizontal "actions" resulting from this frozen-in load case (ISO 19906, 2019). These loads may arise from two primary scenarios: thermal expansion or induced drifting. The former typically does not govern over regular crushing (Määttänen, 2010). A quick hand calculation confirms that for an 8 m monopile the thermal expansion force only exceeds the crushing for ice thicknesses below 0.21 m – assuming a C_R of 0.98 MPa. On the other hand, the induced drifting load case may have an initial large load due to the ice being in full contact with the structure, which is the load case Croasdale described as the intimate contact condition. This condition was partially explored in research referenced by Määttänen (2010), where a trial foundation was placed in the landfast ice zone off the coast of Finland in the Gulf of Bothnia, as shown in Figure 1, with the aim to better understand the design load case of foundations in a land-fast ice zone (Määttänen, 2010). Unfortunately, to the authors' knowledge no articles detailing the results of this research have been published.

Figure 1. Test foundation with real static and dynamic properties of a complete 3 MW OWT installed to the northernmost part of the Gulf of Bothnia (Määttänen, 2010).

Significant driving forces are necessary to initiate movement in a stationary ice sheet, particularly given the added resistance from full-thickness contact. This is especially relevant in scenarios involving complete wind farms with multiple structures acting as anchors. In such cases, the ice may remain stationary for extended periods, leading to a prolonged frozen-in scenario. This, in turn, could affect loads from conventional design load cases (DLCs). Currently, no design standard includes the frozen-in scenario alongside existing DLCs. It is unknown whether this is an intentional exclusion of these load cases. Depending on the thickness and strength of the ice, the frozen-in scenario could act as a (flexible) support,

potentially altering the dynamic characteristics of offshore support structures. To date, this effect has been overlooked, with the primary focus centered on vertical and temperature expansion loads. It is thus necessary to study the implications of such changes to verify no significant design case is disregarded.

ISO 19906 specifies that for the horizontal actions to occur, one of two conditions must be met, one of which is that the structure is situated in an open sea with minimal tidal range and stationary ice persisting for an extended duration (ISO 19906, 2019). This also implies a lack of sufficient driving forces. Notably, the Baltic Sea is known for its minimal tidal water level fluctuations, with reported tidal ranges on the order of centimeters for the Southern Baltic Sea (von Storch et al., 2015; Weisse et al., 2021). Therefore, it is highly probable that the specified condition can be met.

2. Approach

As an initial simplified approach, disregarding the non-elastic nature of ice, the frozen-in scenario was simulated by incorporating two lateral linear springs with a stiffness coefficient, k_{ice}, as depicted in Figure 2, using the aero-elastic software HAWC2 (Larsen & Hansen, 2007). Besides assuming the ice behaves linearly elastic, it is also assumed the ice does not fail throughout the simulations. This allows for an investigation into whether design loads can theoretically become design driving. If this is to be the case, the conditions under which this occurs are postulated as conditions for potential design loads. These ice conditions can then be examined for feasibility of occurring against existing knowledge on ice mechanics. The ice conditions that will be examined are the maximum ice load, the maximum deformation of the ice, and the maximum strain rate the ice is subject to. The strain rate is calculated by assuming a deformation zone of $4D$, where D is the diameter of the evaluated structure, based on research done by Michael & Toussaint (1977). Based on this the strain rate can be found with:

$$\dot{\epsilon} = \frac{V}{4D} \qquad [2]$$

where V is the indentation rate, which is equal to the velocity of the foundation at MSL.

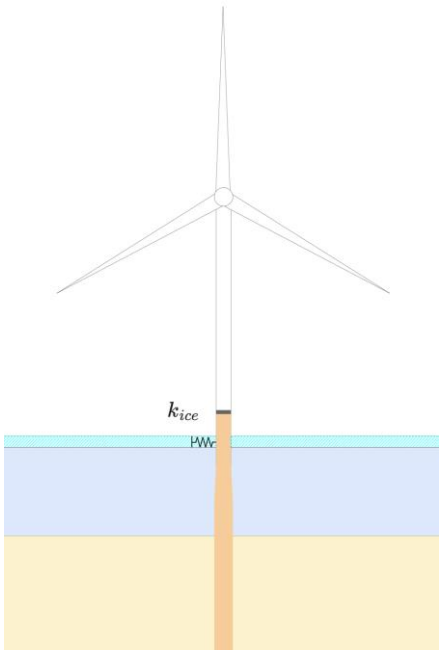

Figure 2. Simplified representation of the frozen-in load case as modelled in HAWC2.

The frozen-in load case is considered as an extension of four existing load cases, three Fatigue Limit State (FLS) and one Ultimate Limit State (ULS). The selected DLCs are summarized in Table 1. All DLCs have been considered unidirectionally with codirectional waves, except in the presence of ice. For ULS the resulting load cases involve start-up and shutdown of the turbine and as selected here, DLC1.4: the extreme coherent gust and direction change. Due to the increase of RNA masses in recent years the transient effect of this load case can be a driving factor for the overturning moment at the interface of the foundation. The presence of ice may affect these loads due to the increased effective stiffness around waterline.

Table 1. Considered Design Load Cases as listed by IEC 61400-3-1 (2019).

DLC	Description	Type	Wind speed (v_{hub})
1.2	Power production	FLS/ULS	$v_{\mathrm{in}}<v_{\mathrm{hub}}<v_{\mathrm{out}}$
1.4	Power production (Extreme coherent gust + direction change)	ULS	v_{rated}
6.4	Parked (Standing still or idling)	FLS/ULS	$v_{\mathrm{hub}}<v_{\mathrm{in}}$ $v_{\mathrm{in}}<v_{\mathrm{hub}}<v_{\mathrm{out}}$
7.2	Parked and fault conditions	FLS/ULS	$v_{\mathrm{hub}}<v_{\mathrm{hwo}}$

Asides from the effect of being frozen-in on ULS, the impact of FLS is investigated. Since the FLS are largely driven by hydrodynamic loading of the waves, the fatigue loads are expected to reduce in the frozen-in load case in which waves or not present. However, to isolate the effect on fatigue damage due to the increased stiffness of the frozen-in load case, the simulations are also run with waves for comparison – despite this not being a naturally occurring load case. It is expected that both the increased stiffness and the exclusion of waves will positively affect the Damage Equivalent Moment (DEM), meaning it will reduce over the entire foundation. Currents were excluded from this study as the research focused on comparison between two scenarios, including current would not have changed said comparison as it would be included as equal constant forcing.

A parameterized LCT for a representative (fictitious) project site in the Baltic Sea was established based on industry experience, formulated through Equations 2-4:

$$H_s = 8.18 \times 10^{-8}\, v_{\mathrm{hub}}^6 - 9.13 \times 10^{-6}\, v_{\mathrm{hub}}^5 + 3.86 \times 10^{-4}\, v_{\mathrm{hub}}^4 - 7.87 \times 10^{-3}\, v_{\mathrm{hub}}^3 + 8.25 \times 10^{-2}\, v_{\mathrm{hub}}^2 - 1.86 v_{\mathrm{hub}} + 5.90 \quad \textbf{[3]}$$

$$T_p = 4.27 \times 10^{-3}\, H_s^5 - 9.95 \times 10^{-3}\, H_s^4 + 8.91 \times 10^{-1}\, H_s^3 - 3.80 \times 10^{-3}\, H_s^2 + 8.14 \times 10^{-2}\, H_s + 1.20 \quad \textbf{[4]}$$

$$I = 71.75\, v_{\mathrm{hub}}^{-0.704} \quad \textbf{[5]}$$

Where v_{hub} is the wind speed at hub height, H_s is the significant wave height, T_p is the associated wave peak period and I is the turbulence intensity. The water depth of the site was set to 36 meters.

The LCT as described in Table 1 sums to 120 simulations. The simulations are executed for six ice stiffnesses ranging from 0 to 375 MN/m, with increments of 75 MN/m. Additionally, simulations are performed both with and without waves, resulting in a total of 1440 executed simulations. The selection of the listed ice stiffnesses is revisited in the discussion.

The IEA 15 MW turbine was selected with its associated tower downscaled from 10 to 8 meters at tower interface – in line with industry standard – while maintaining its D/t ratio. A foundation was generated using Wood Thilsted's foundation design framework MORPHEUS, described in Nielsen et al. (2022).

4. Results – Dynamic behavior

The frozen-in scenario, as modelled by the lateral springs, resulted in an increase in the stiffness of the first and second fore-aft (F-A) and side-side (S-S) modes as shown in Figure 3. The increase tapers off as the stiffness increases, as with increasing stiffness the spring effectively becomes a support. For the first mode the maximum increase, which corresponds to a rigid support at MSL, was approximately 22% in both directions, while for the second mode it was 39 and 44% for F-A and S-S, respectively. The impact of the spring at the waterline is substantially larger for the 2nd mode, which is explained due to the large mode shape amplitude at waterline for this mode. Besides frequencies, Figure 3 provides the associated linearized foundation stiffness based on initial stiffness for a concentrated load at ice action point, $k_{s;0}$. In line with expectations, the foundation stiffness as the ice stiffness increases. Note, the ice stiffness has been normalized with $k_{s;0}$.

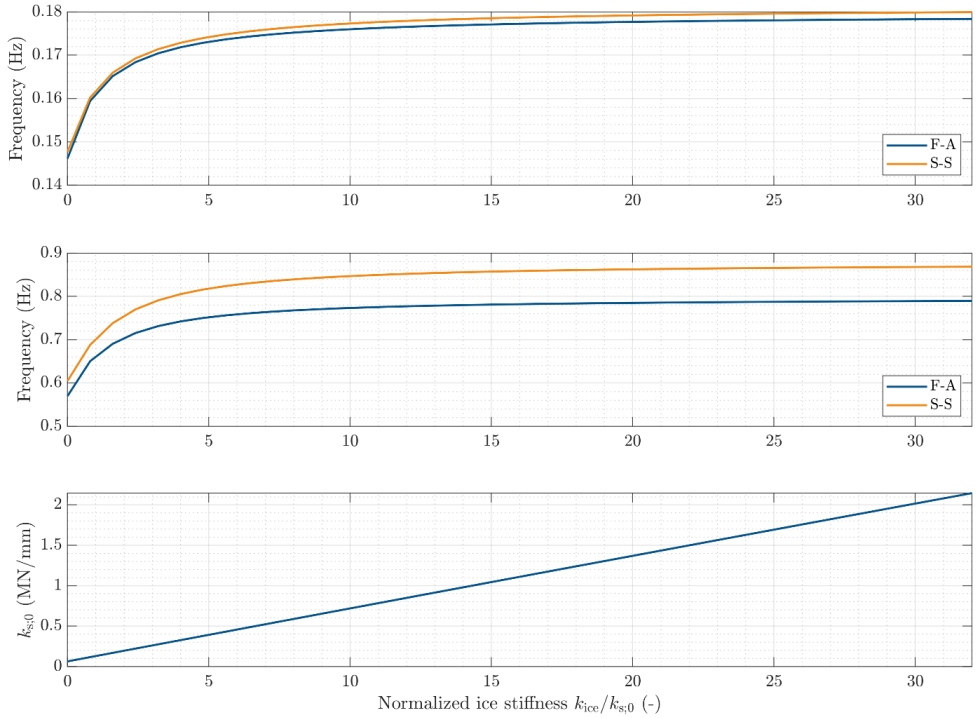

Figure 3. Natural frequency of the 1st F-A mode (top), 2nd S-A mode (middle), and flexibility parameter (bottom) as a function of normalized ice stiffness.

Figure 4 illustrates the spectral plot showing the wave spectra of the load case table, the 1P and 3P regions, and the minimum and maximum first natural frequencies of the structure from Figure 2. Based on the distribution of energy in Figure 4, it is expected that the increased frequency would not adversely affect the offshore wind turbine. The range of ice stiffnesses selected for simulations are in the range where small stiffnesses increase have a large impact on the resulting frequency.

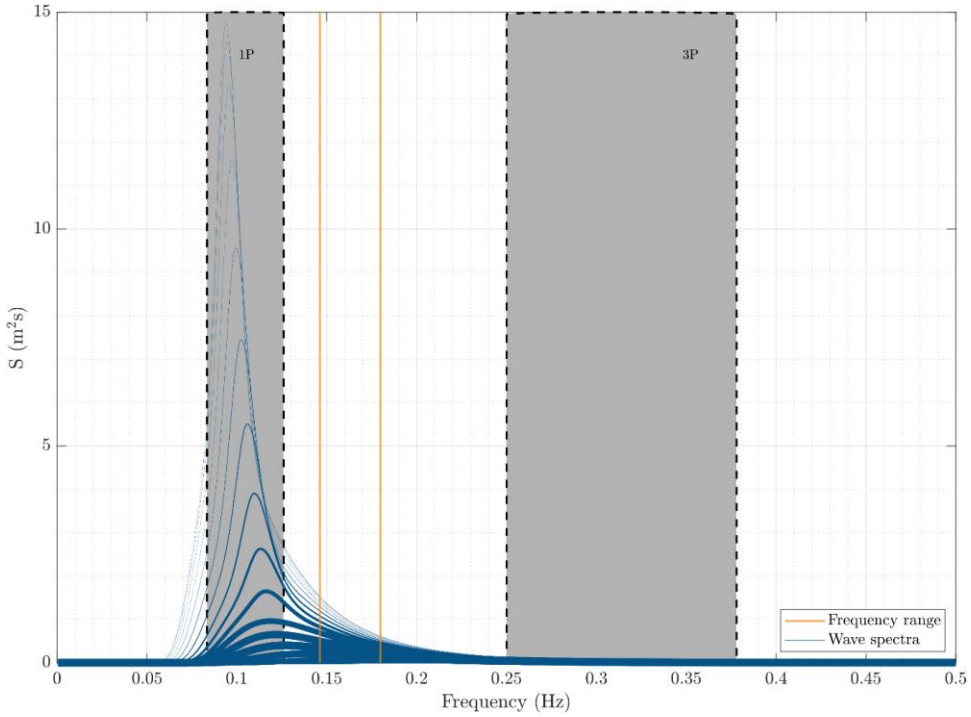

Figure 4. Spectral plot of the turbine 1P and 3P regions, the calculated lower and upper limit of the first F-A and S-S mode, and the simulated sea states weighted based on their probability.

5. Results – Loads and kinematic behavior

The results of the simulations are provided in terms of foundation loads, by presenting load envelopes along the full structure down to the seabed, alongside interface moments, shear forces, and damage equivalent moments (DEMs) plotted against varying ice stiffnesses. All presented load envelopes, interface and MSL loads, are provided for the ice-free condition or for ice without waves, as these are tangible physical load cases. The ice conditions are given as maximum ice load, maximum deflection at mean sea level (MSL) and the maximum strain rate of the ice for all simulated ice stiffnesses.

Figure 5 shows the ULS load envelope of the overturning moment and shear for the entire structure, for all considered ice stiffnesses. The effect of the frozen-in condition is very pronounced from MSL downwards as shown by the kink and the abrupt increase in the load profile of the overturning moment and shear, respectively. For the overturning moment, the 'regular' or ice-free condition (k_{ice}= 0) is governing for all elevations, and for increasing ice stiffness, the magnitude of the envelope reduces. An opposite trend is observed for the shear envelopes, showing that the shear from MSL and below increases for higher ice stiffnesses. Shear below MSL is approximately constant for the frozen-in load case, due to the absence of waves.

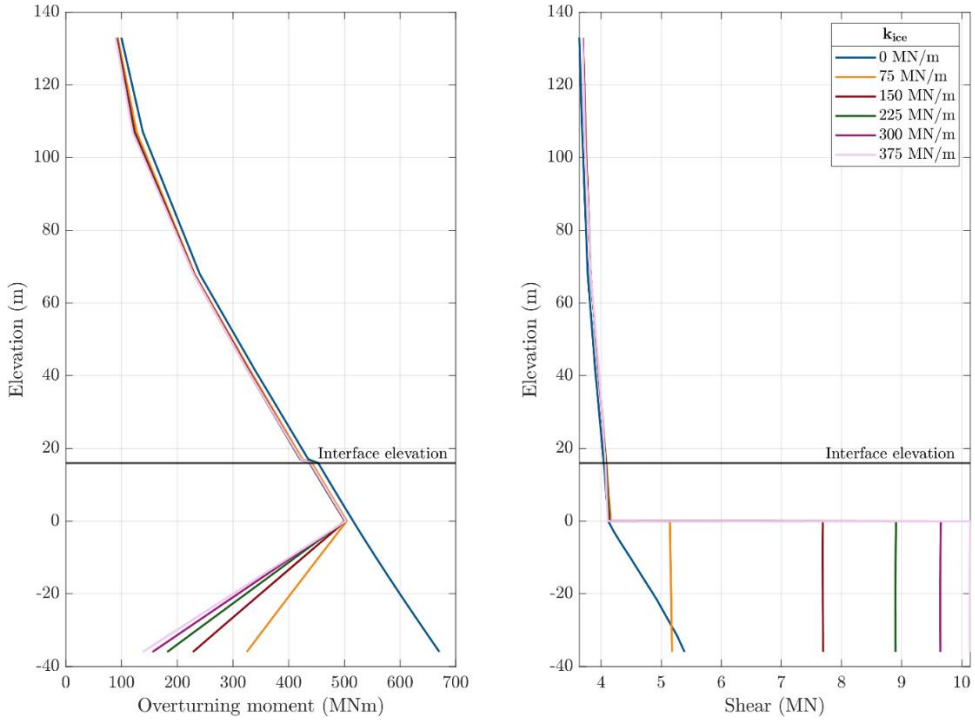

Figure 5. Overturning moment (left) and shear (right) load envelopes for DLC 1.4 over the length of the full tower and foundation for all simulated ice stiffnesses.

Figure 6 presents a comparison of interface and MSL loads for DLC 1.4. The loads for all ice stiffnesses are normalized with respect to $k_{s;0}$. Interface moments are observed to be highest for the ice-free condition without ice, whereas the shear increases from approximately 4 to 10 MN with increasing ice stiffness.

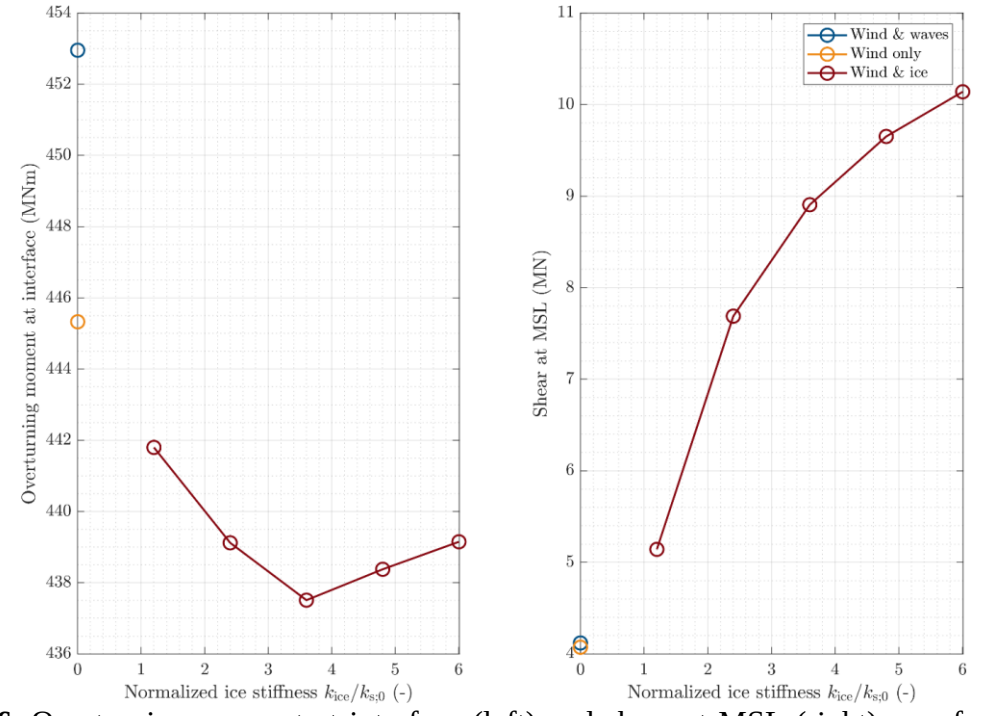

Figure 6. Overturning moment at interface (left) and shear at MSL (right) as a function of normalized ice stiffness for all simulated cases.

Comparable plots are provided in Figure 7 for DEMs contributing to the fatigue damage. The highest reported DEM is observed in the scenario with waves but without ice.

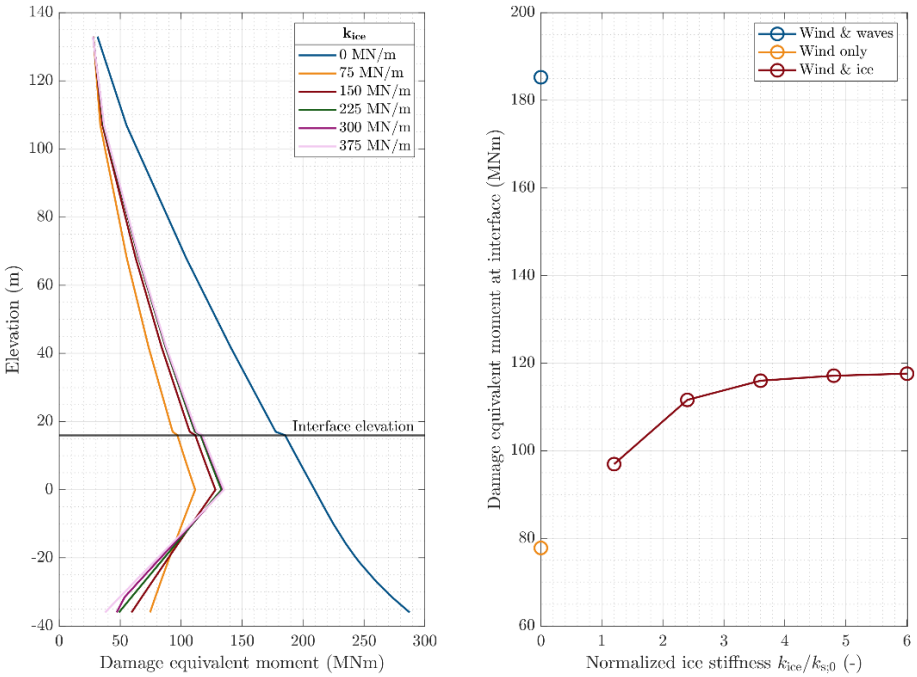

Figure 7. DEM over the length of the full tower and foundation for all simulated ice stiffnesses (left) and DEM at interface as a function of normalized ice stiffness for all simulated cases (right).

Figure 8 illustrates the worst conditions – in terms of load, deformation, and strain rate – the ice is subject to during the frozen-in load case. The maximum observed ice load increases from 6.7 up to 10.5 MN between 75 and 375 MN/m ice stiffness. The maximum deflection at MSL decreases from 0.089 to 0.027 m over the same range. Similarly, the strain rate decreases from 0.09 to 0.35 s^{-1}.

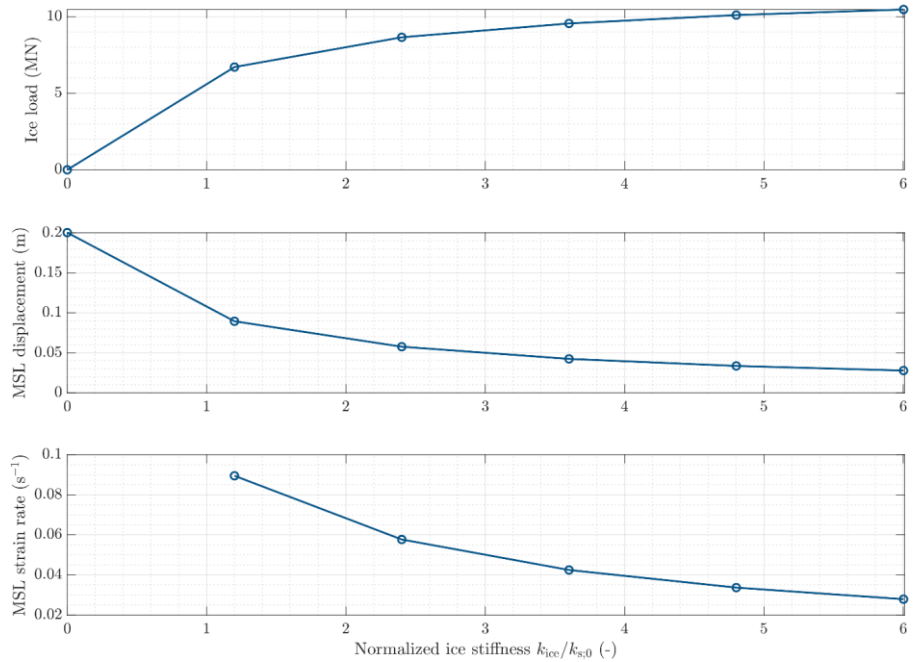

Figure 8. Three ice conditions as a function of normalized ice stiffness. From top to bottom: maximum ice load, maximum deformation at MSL and maximum strain rate in the ice.

4. Discussion

The results indicate a decrease in overturning moment and a substantial increase in shear forces during the frozen-in load case for the ultimate limit state (ULS). This reduction in overturning moment was consistently observed regardless of whether waves were considered in the frozen-in simulations or not. Furthermore, the presence of waves did not influence the observed increase in shear forces. These findings are in line with expectations, as the significant overturning moment stems from the transient effect of the large RNA mass displacing during extreme coherent gusts, which is not adversely affected by the increased ice stiffness. However, the sudden large displacement of the RNA forces the structure further into the surrounding ice. As a result, since the ice is modeled as a linear spring, this imposes a considerably larger shear force on the structure at MSL.

Typically, in wind-dominated load cases, the shear profile is not significant, whereas in wave-dominated scenarios, it tends to increase considerably between MSL and the sea floor. While the impact of shear is generally considered less significant from a design standpoint, a notably higher shear and slightly lower overturning moment could potentially govern the design of the foundation. Particularly, sections of the foundation just below MSL experience significantly higher shear compared to ice-free load cases, as the shear typically increases to large values along the length rather than instantly. To investigate this, the ULS utilizations are calculated based on the yield and buckling checks in accordance with EN 1993-1-6 (EN 1993-1-6, 2007). The resulting utilizations at interface, MSL, and seafloor, are presented in Table 2.

Table 2. ULS utilization at interface, MSL and seafloor.

Ice stiffness	Utilization (-)		
	Interface	MSL	Seafloor
k_{ice}= 0 MN/m	0.56	0.60	0.54
k_{ice}= 75 MN/m	0.55	0.64	0.30
k_{ice}= 150 MN/m	0.55	0.64	0.23
k_{ice}= 225 MN/m	0.54	0.64	0.20
k_{ice}= 300 MN/m	0.55	0.64	0.19
k_{ice}= 375 MN/m	0.55	0.64	0.17

The results, as partially outlined by Table 2, indicate that for specific elevations below MSL the ULS utilization is governed by the frozen-in load case, originating from the extreme buckling check. This confirms that, according to the current methodology assuming a linear elastic non-failing ice sheet, the frozen-in load case cannot be disregarded.

The assumption of a linear elastic ice model without failure represents a significant oversimplification. Ice exhibits plastic and delayed-elastic deformations occur at low strain rates, which may reduce the loads. Additionally, a failure threshold would impose limitations on the maximum reported ice load, which is directly related to the observed shear force. Incorporating both these effects is required to assess if the frozen-in load case may be governing or results from an oversimplified representation of reality. Given the marginal increase in ULS utilization, it is expected that an improved modelling of the ice would reduce the observed ice loads. To capture the frozen-in load case's impact, an existing ice model capable of reproducing ice behavior could be expanded to two dimensions while enforcing complete initial contact with the structure.

Besides the obvious assumptions listed above, the model also neglects bending effects, despite theoretical analyses indicating that the resistance moment of the ice cover to bending formations should be considered, as highlighted by Kerr (1984). It is important to note that Kerr's conclusions were drawn based on piles considerably smaller relative to a monopile. Therefore, future research should investigate the applicability of these conclusions to larger structures such as monopiles, along with the other specified assumptions.

For FLS the frozen-in scenario reduces the fatigue damage significantly. The minimal observed reduction was 30% for the highest considered ice stiffness of 375 MN/m. By running the simulation with and without wave loads the origin of the reduction was investigated. It was confirmed that both the increased stiffness at the waterline and the absence of waves are beneficial for the resulting fatigue damage in the frozen-in load case, yielding lower FLS damage. The reduction is partly due to the stiffer response of the foundation resulting from the spring at MSL. The other reason for the reduction in DEM is due to the absence of waves. As ice stiffness increases, the contribution of wave loading to the DEM diminishes, as the foundation becomes increasingly rigid between MSL and sea floor.

Besides the impact on loads, the conditions the stationary ice is subject to, were investigated. The results can be scrutinized to determine the feasibility of the frozen-in load case to be 'naturally' occurring, i.e. will the stationary ice remain intact during the load case? For this, three conditions must be met by the ice: strength, deformation, and strain rate condition. The ice must have sufficient strength to resist the imposed load by the offshore wind turbine leading up to and during the extreme event. Similarly, it must be able to deform elastically – without failing – given a particular strain rate. For an ice stiffness of 375 MN/m, the conditions this ice sheet would have to resist are 10.5 MN load, 0.027 mm deformation, and a strain rate of 0.35 s^{-1}. The assumed deformation zone in the strain rate relation, given by Equation 2, can be applied to find an indicative relation for ice stiffness as a function of ice thickness:

$$k_{ice} = \frac{EA}{4D} = \frac{EhD}{4D} = \frac{Eh}{4} \quad [6]$$

Where E is the elastic modulus of ice, which is equal to 3 GPa, and h is the ice thickness. For ice thicknesses between 0.1 and 0.5 m Equation 6 yields the ice stiffnesses simulated in the current research. However, the provided relation for the deformation zone is based on model tests with ice plates of 81 by 81 cm for ice thicknesses between 2.5 and 10 cm, and stationary in-field ice sheets may yield very different stiffnesses for similar ice thicknesses. Nonetheless, in lieu of more data, this relation is considered for further deliberations. Consequently, an ice thickness of 0.5 m would need to resist 10.5 MN of imposed load.

To determine whether the stationary ice can withstand the imposed loads, the prevalent failure mechanism during the frozen-in load case needs to be known. Initial investigations in 1975 showed that for frozen-in piles failure occurred due to tensile strain, over shear or compression failure (Hirayama, 1975). However, this only mentions the initial failure. The full breakout phenomenon of a structure in fast ice was examined in a study by Tatsura (1988). It confirmed that tensile failure does occur first at the backside of the structure, but it is followed by shear failure – in line with the movement – on both sides of the pile and finally compression failure in front of the pile. They also note that even though the tensile and shear failure occur first, the compression failure is critical for the horizontal load, and they report an associated maximum break out load approximately two to three times larger than the crushing load. Tatsuta argues that the confinement in vertical direction creating a triaxial stress condition (Tatsuta, 1988).

The initial investigations in 1975 also made mention of a different failure due to the locally thicker ice (Hirayama, 1975). Based on this research it seems likely, that separation between ice and structure would take place during the frozen-in load case. The displacements of the monopiles at MSL would result in tensile failure on both sides of the ice. However, despite separation, the imposed load could still be substantial due to the subsequent compressive failure.

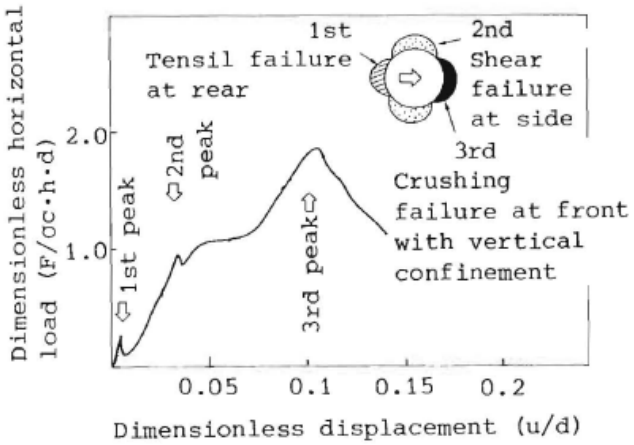

Figure 9. Load displacement curve during break out test (Tatsuta, 1988)

If the ice stiffness of 375 MN/m is assumed to be corresponding to an ice thickness of 0.5 m the required global 'compressive strength' to resist the 10.5 MN is roughly 2.63 MPa. Based on a review of properties of sea ice, estimates of the uni-axial compressive strength for full thickness ice are in the range of 0.4-5 MPa for strain rates from 10^{-7} to 10^{-4} s^{-1}, respectively (Timco & Weeks, 2009). For higher strain rates, as observed in the current research, it is not entirely clear, but during laboratory tests even higher compressive strength was reported (Jones, 1997). Hence it is likely, under the given assumptions, the ice thickness can resist the maximum load during power production. Contrary, it remains uncertain whether the ice can withstand the reported maximum deformation of 2.7 cm, which likely requires delayed-elastic or viscous deformations in which case the modelling would have to be adapted.

Furthermore, the assessment of the frozen-in load case requires a practical examination – is sufficient ice growth possible around vertical structures with continuous displacements in the waterline? This can be assessed by evaluating the 'typical' displacements at MSL during power production. Figure 10 provides insight in this for both the wave and ice conditions. It illustrates the probability of a peak MSL displacement exceeding a specific value, derived from a random rainflow counted cycle analysis of the displacement time series. The analysis indicates that the majority of MSL displacement peaks fall within a narrow range (< 5 cm).

Prior studies have highlighted the dependency of ice formation around structures on various factors, including structural temperature, water salinity, structural roughness, and kinetics of ice formation (Sackinger & Sackinger, 1977). However, ice formation under sustained in-plane motion is less understood. Nevertheless, research has shown that gradual formation of fast ice remains feasible despite potential cracks resulting from tidal fluctuations, and, if formed, such ice would likely exhibit uniform and continuous characteristics (Sackinger & Sackinger, 1977). Whether similar characteristics are observed under horizontal oscillations requires further research.

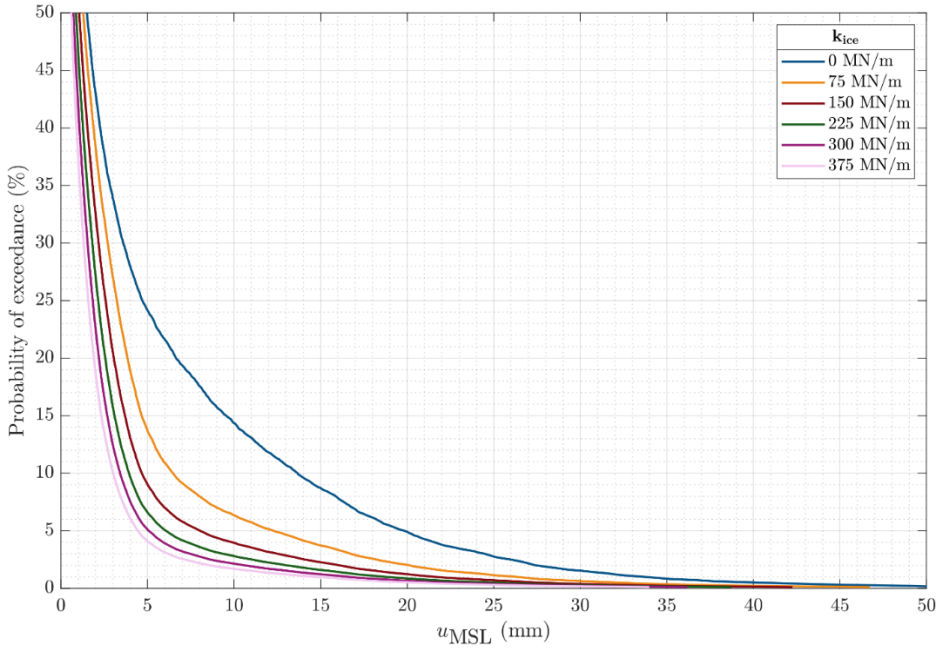

Figure 10. Probability of exceedance for MSL displacements during power production for all simulated ice stiffnesses.

5. Conclusion

An initial investigation was conducted into the load effects of the frozen-in load case, in which stationary ice fully engulfs an offshore wind farm. A simplified model was applied, assuming the ice to behave linearly elastic and to remain intact. For these assumptions, the frozen-in load case does not lead to an increase in overturning moments or damage equivalent moments for offshore (monopile) foundations. However, shear loads between MSL and sea floor were shown to increase substantially, which yields higher utilizations for a few foundation sections below MSL. This study also investigated the conditions the ice would be subject to in such an extreme event leading to higher design shear in the foundation. The results of the numerical simulation with a simplified model defined conditions for the fast ice to remain intact. Ice with an ice stiffness of 375 MN/m was shown to need to resist 10.5 MN while elastically deforming 0.027 m during an extreme event. These orders of magnitude are considered on the upper range of realistic values for sea ice to fail in compression. A more detailed material model for the frozen-in condition is required to assess how delayed-elastic and viscous deformation components play a role over time. Such a model could aid in determining whether the observed increase in utilizations stems from oversimplification, as is expected, or reflects actual physical phenomena. Due to the non-conservativism of ignoring the frozen-in load case, such a study adds significant relevance.

References

Adachi, H., Yashima, N., Nakanishi, M., Niki, H., & Ikezawa, Y. (1988). Earthquake response characteristics of offshore structures in the presence of ice floes. *Proceedings of the 9th IAHR International Symposium on Ice*.

Christensen, F. T., & Tryde, P. (1984). Extraction of piles by repeated water level fluctuations. *Proceedings of the 8th IAHR International Symposium on Ice*.

Christensen, F. T., & Tryde, P. (1986). Uplifting ice forces on long vertical walls. *Proceedings of the 8th IAHR International Symposium on Ice*.

Croasdale, K. R. (1975). Ice forces on marine structures. *Proceedings of the 3rd IAHR International Symposium on Ice Problems*.

EN 1993-1-6. (2007). *Design of steel structures: strength and stability of shell structures: Vol. Part 1-6*. BSI.

Hammer, T. C., Willems, T., & Hendrikse, H. (2023). Dynamic ice loads for offshore wind support structure design. *Marine Structures*, *87*. https://doi.org/10.1016/j.marstruc.2022.103335

IEC 61400-3-1. (2019). *Wind energy generation systems - Part 3-1: Design requirements for fixed offshore wind turbines* (Edition 1.).

Inoue, M., & Frederking, R. (1986). Adhesion strength of piles in saline ice. *Proceedings of the 8th IAHR International Symposium on Ice*.

ISO 19906:2018(E). (2018). *Petroleum and natural gas industries - Arctic offshore structures (draft for WG8 review)*.

Kerr, A. (1975). Ice forces on structures due to a change of the water level. *Proceedings of the 3rd IAHR International Symposium on Ice Problems*.

Kerr, A. (1984). Analysis of piles frozen-in to an ice cover and subjected to forces that cause bending. *Proceedings of the 8th IAHR International Symposium on Ice*.

Kerr, A., & Stafford, A. (1986). Ice forces on a circular pier due to water level changes, with partial flooding. *Proceedings of the 8th IAHR International Symposium on Ice*.

Larsen, T. J., & Hansen, A. M. (2007). *How 2 HAWC2, the user's manual*. Risø National Laboratory.

Määttänen, M. (2010). *Ice research and engineering in Finland*.

Ohtsuki, F., Koichi, S., Kazuyuki, S., Kohki, S., Toshiyuki, O., & Hiroshi, S. (1988). A experimental study on adfreeze bond strength of sea ice to heavy-duty coated steel pipe piles. *Proceedings of the 9th IAHR International Symposium on Ice*.

Sackinger, W. M., & Sackinger, P. A. (1977). Shear strength of the adfreeze bond of sea ice to structures. *Proceedings of the 4th International Conference on Port and Ocean Engineering under Arctic Conditions*.

Sodhi, D. S. (1988). Ice-induced vibrations of structures. *Proceedings of the 9th IAHR International Symposium on Ice*, 625–657. https://www.iahr.org/Portal/About_US/Technical_Division/Ice_Research_and_Engineering_Committee.aspx

Terahima, T., Nakazawa, N., Kioka, S., Usami, N., & Saeki, H. (2006). Vertical ice forces on pile structures under water level changes. *Proceedings Oh the 18th IAHR International Symposium on Ice*.

von Storch, H., Jiang, W., & Furmanczyk, K. K. (2015). Storm surge case studies. In *Coastal and Marine Hazards, Risks, and Disasters* (pp. 181–196). Elsevier Inc. https://doi.org/10.1016/B978-0-12-396483-0.00007-8

Weisse, R., Dailidiene, I., Hünicke, B., Kahma, K., Madsen, K., Omstedt, A., Parnell, K., Schöne, T., Soomere, T., Zhang, W., & Zorita, E. (2021). *Sea level dynamics and coastal erosion in the Baltic Sea region*. https://baltic.earth